ELSEVIER

Journal of Power Sources 68 (1997) 139–144

JOURNAL OF POWER SOURCES

Microvoltammetric studies on single particles of battery active materials

Isamu Uchida *, Hironobu Fujiyoshi, Shinichi Waki

Department of Molecular Chemistry and Engineering, Faculty of Engineering, Tohoku University, Aramaki-Aoba, Aoba-ku, Sendai 980-77, Japan

Accepted 14 October 1996

Abstract

This paper demonstrates the unique features of microvoltammetric techniques to investigate the solid-state electrochemistry of battery materials. It is shown that single particles having 10 μm sizes were successfully made into the working electrode. Microvoltammograms for $LiCoO_2$ and spinel-related manganese oxides were measured at various sweep rates and their kinetic features were examined. © 1997 Published by Elsevier Science S.A.

Keywords: Microelectrodes; Lithium secondary batteries; Cathode materials; Lithium cobalt oxide; Spinel-related manganese oxides; Cyclic voltammetry; Microvoltammetry

1. Introduction

Battery active materials, usually in powdered form, are mixed with an organic binder and a conductive additive, and then they are subjected to charge/discharge tests under constant current for performance evaluation. This is a conventional way for material searching, giving information on quasi-static capacity. In general, electrodes consisting of those materials are a type of composite electrodes with high surface area (porous electrodes), and we have to be careful in the determination of kinetic parameters such as diffusion coefficients when applying electrochemical transient techniques and a.c. impedance methode. It is also pointed out that the complete electrolysis of redox composite takes considerable long time because of low diffusion coefficients inside the solid phase.

Microelectrode techniques are very versatile in kinetic studies because of high rates of diffusion flux, less interference by resistive polarization and capacitive currents due to the double-layer capacity; they are suitable for measurements of a small environment such as biological cells [1–3]. So far there have been some works studied by microelectrode techniques in the battery field, reporting the determination of electrochemical windows in several organic solvents [4], the analyses of mass transport and kinetic parameters for lithium deposition/dissolution [5–8]. Recently Bursell and Björnbom [9] applied a microelectrode technique to characterize single carbon agglomerate particles of size ranging form 50 to 120 μm in an alkaline solution. This technique consisting of micromanipulation of a fine carbon filament to make an electric contact with a single particle has been found to be very useful to study battery active materials with a powdered form [10], because it allows us to obtain the straightforward current/potential behavior of the sample particle itself without any dilution due to a binder and conductive assistant.

The micromanipulation of microelectrodes in vivo systems is a established technique [11,12] and amperometric measurements have been carried out for cell aggregations such as brain tissues [13,14] and giant cells [15]. Previously, we developed a microelectrode setup capable of measurements of intercellular voltammetry where the tip of microelectrode was inserted into single cells of several ten μm, and demonstrated the microvoltammetry inside living single cells with ultramicroelectrodes of Pt/Ag [16] and Pt/carbon [17]. Based on this setup, we established a new technique targeting a single particle for characterization of the solid-phase electrochemistry of battery materials and determined the apparent hydrogen diffusion coefficients in $LaNi_5$ and Pd [10] and in some metal hydrides, the AB_5 type alloys ($LaNi_{4.5}Al_{0.5}$ and $LmNi_{4.0}Co_{0.4}Mn_{0.3}Al_{0.3}$) and the C15-type Laves phase alloys ($ZrNi_{1.4}$, $ZrMn_{0.6}Co_{0.1}V_{0.2}Ni_{1.2}$ and $ZrMn_{0.4}Cr_{0.4}Ni_{1.2}$) [18] in alkaline solutions by the potential step method.

* Corresponding author.

PII S0378-7753(96)02623-7

In the present work, we extended our technique to redox oxide particles in aprotonic organic solvents and made microvoltammetric studies of $LiCoO_2$ and spinel type $LiMn_2O_4$, which is of particularly interest in redox behavior because it shows well defined two peaks and changes greatly its voltammogram depending on addition of the fourth element. This paper demonstrates the unique features of the microelectrode technique to investigate the solid-state electrochemistry of battery active materials.

2. Experimental

The electrochemical setup is shown in Fig. 1(A). In this experiment, a Pt–Rh fine filament (diameter: 25 μm) was employed as a current collector as shown in Fig. 1(B). The filament was coated with a thin film of Teflon to minimize a background current, then it was mounted into a glass tubing and held by an *X–Y–Z* micropositioner (Oyama, OYM-130). The tip of the filament was contacted with a particle spread on a disk of glass frit or a separator sheet soaked with electrolyte solutions by handling the micropositioner and an electric *X–Y–Z* stage (Chuoseiki, Model M9103), on which a small Petri dish containing particles and the reference electrodes was placed, and a target particle was focused on with a stereo microscope (Nikon SMZ-U) with an enlargement of about ×500. The dimension of particle was determined by an optical image obtained under a micrometer eyepiece. Except the microscope, the cell assembly including the *X–Y–Z* stage was placed in a small dry box filled with dry argon and the micromanipulation of the filament was carried out by a remote controller outside the box. Experiments were carried out at room temperature.

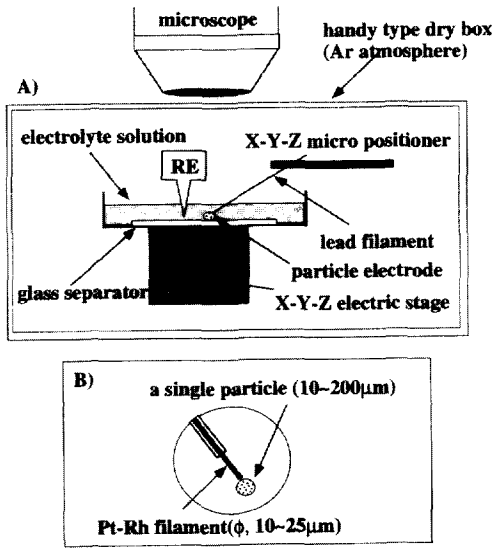

Fig. 1. Schematic illustration of (A) the measurement system and (B) illustration of a single particle electrode.

All electrochemical measurements were carried out with a potentiostat (Hokuto Denko, Model HA-150) coupled with a slow potential scanner (Hokuto Denko, Model HB-104). The reference electrode was a lithium foil, and electrolyte solutions were 1 M $LiClO_4$/propylene carbonate (PC) and 1 M $LiClO_4$/PC + ethylene carbonate (EC).

The oxides used in this work were prepared by a wet process called the citrate process [19]. This process is based on the thermal decomposition of precursors with high homogeneity. The precursors were obtained by vacuum drying the citrate complex derived from the solution mixture of citric acid, lithium nitrate and transition metal nitrate; one mole of lithium nitrate and one mole of cobalt(II) nitrate were dissolved in a solution of two moles of citric acid for the preparation of $LiCoO_2$ and it was dried in a rotary evaporator at 60–80 °C. For the preparation of $LiMn_2O_4$, the molar ratio, 1(Li nitrate):2(Mn(II) nitrate):3(citric acid) was used. The precursor was decomposed at 300 °C, then heated to 700°C under oxygen. Thermal gravimetric analyses were carried out for the heating process of precursors, and the oxides thus obtained were characterized by X-ray diffraction analysis. We confirmed the single phase of $LiCoO_2$ (hexagonal; $a = 2.813$ Å, $c = 14.029$ Å) and the single phase of $LiMn_2O_4$ (cubic; $a = 8.226$ Å).

3. Results and discussion

3.1. Microvoltammetry of $LiCoO_2$

Since battery active materials are usually prepared in the form of powder, it would be of a great advantage, if we can make a single particle to be the working electrode without any conditioning. However, reducing the particle size to a μm range, we have to measure currents of nano-ampere (nA) levels, as shown in Fig. 2. It shows three peaked, reversible CVs, which were obtained at $LiCoO_2$ particles with different diameters ranged from 7 to 16 μm at the scan rate = 10 mV/s. This experiment demonstrated that 10 μm size particles have been successfully made into the working electrode. The peak current should be proportional to the particle surface area if the current is limited by the mass transfer. Assuming that the selected particles are spheres, then the peak current is proportional to the square of the particle diameter. This relationship was confirmed as shown in Fig. 3.

Currents observed in the microvoltammetry are of nA levels, at least 3 to 5 orders smaller than in usual cyclic voltammetry, because of the small surface area of the particle electrode. This feature greatly improves the distortion of CV behavior due to an *iR* drop. Even if we use high resistive

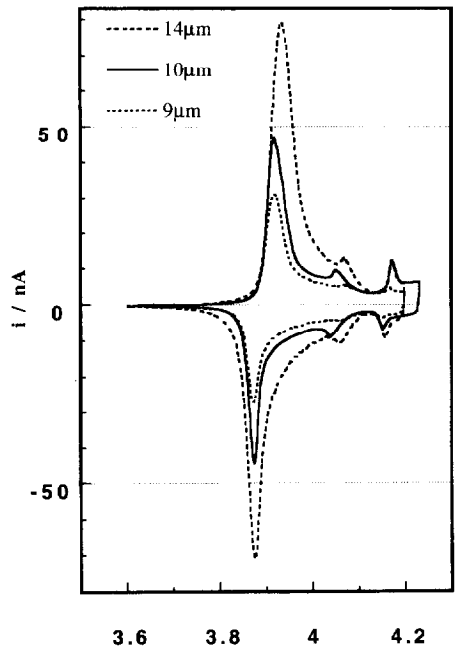

Fig. 2. Cyclic voltammograms for $LiCoO_2$ particles with different particle sizes, obtained at the second cycle at 10 mV/s in 1 M $LiClO_4$/PC + EC.

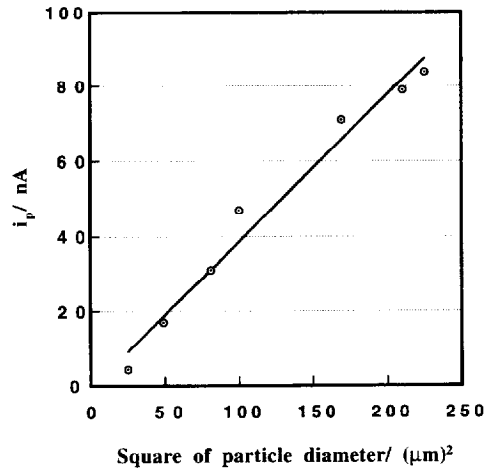

Fig. 3. Plots of the peak current vs. square of the particle diameter. The experimental conditions are same with those of Fig. 2.

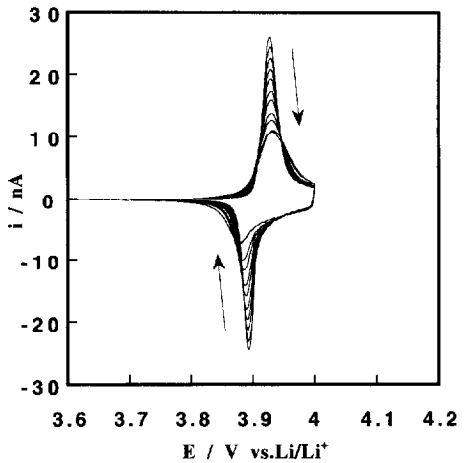

Fig. 4. Cyclic voltammograms for a single particle $LiCoO_2$ (diameter: 13 μm), obtained by continuous potential cycling (cycle number 2 to 50) at 3 mV/s between 3.6 and 4.0 V vs. Li/Li^+.

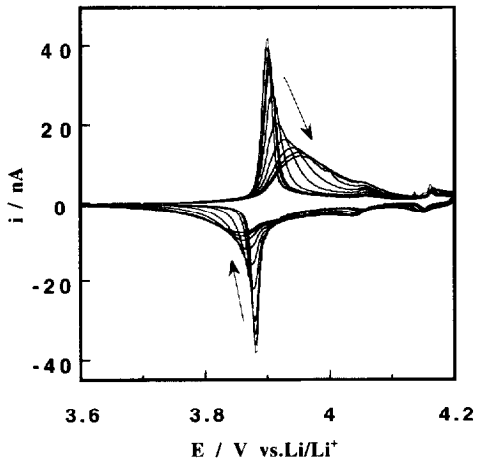

Fig. 5. Cyclic voltammograms for a single particle $LiCoO_2$ (diameter: 18 μm), obtained by continuous potential cycling (cycle number 2 to 30) at 3 mV/s between 3.6 and 4.2 V vs. Li/Li^+.

materials without conductive additives, we can minimize the *iR* effect on CV in the usual sweep rates, 1–10 mV/s. This is advantageous in the characterization of the CV behavior; typical peak potentials obtained with a sweep rate of 3 mV/s, E_A, E_B and E_C, are equal to 3.904, 4.058, and 4.163 V versus lithium, respectively. Comparing the results with those obtained with a thin film $LiCoO_2$ [20] and calculated from the derivative $-dx/dV$ [21], we found that the above peak positions are in good agreement with them. This confirms that this technique gives correct responses of the Li^+ ion extraction/insertion process in cyclic voltammetry.

Considering that this size of particle can be entirely oxidized/reduced during the potential cycling at $\nu = 1$–10 mV/s, we can regard the multiscan cyclic voltammetry as an accelerated test of cyclic performance. One cycle of the potential scanning at $\nu = 10$ mV/s needs only 200 s for covering a 1 V potential range. If we use 1 mV/s, it takes about 30 min for one cycle; it may be ten times faster than that of the normal cycling test. Figs. 4 and 5 show CVs obtained by continuous scanning (2–50 cycles at 3 mV/s) reversed at different potentials, $E_\lambda = 4.0$ and $E_\lambda = 4.2$, to examine the reversibility and the cycle stability. It was found that the kinetic reversibility strongly depends on the reverse potential; the reversibility was highly preserved in the case of $E_\lambda = 4$

V, because the peak potential did not shift appreciably during the potential cycles. On the other hand, large potential shift was observed with increasing the reverse potential to 4.2 V, indicating some kinetic deterioration brought about by the potential cycling. Similar behavior was pointed out in constant current charge/discharge experiments by Ohzuku and Ueda [22]. The peak currents also rapidly decreased with cycling, and some irreversible changes in physicochemical properties associated with the crystal structure must be involved. According to our experience, this cycle stability was quite sensitive to the sample preparation and the water content in the organic solvent. Further study is now under way in this respect.

From the viewpoint of kinetics it is interesting to examine the half-peak width of CV and the relationship between the peak current and the sweep rates. The half-widths of the main peak (A) in Fig. 4 were narrow, ranged from 20 to 45 mV, depending on the cycle number. The peak current was a linear function of the sweep rate in a limited range lower than 3 mV/s. At higher sweep rates, however, it deviated from the linear relationship, being close to a square root relationship. It should be noted that the mass-transfer process of the lithium ion in the solid phase controls the current behavior. According to the theory of mass transfer in a homogeneous phase where activities can be replaced by mole fractions, i.e., an ideal solid solution case, the i–E curves should be symmetrical with a half-width of about 90 mV for $n=1$ [23] and 180 mV for $n=0.5$ [24]. Our data indicate rather narrow half-widths and this discrepancy can be ascribed to a two-phase oxidation reaction. According to XRD studies, Reimers and Dahn [21] reported a two-phase coexisting region in the region $0.75<x<0.93$, and Ohzuku and Ueda [22] reported a topological two-phase reaction for $0.75<x<1$. The main peak (A) in the CV is probably corresponding to this region.

3.2. Microvoltammetry of $LiMn_2O_4$

As discussed in the foregoing section, the small particle experiment is useful to kinetic studies of intercalation processes as well as rapid evaluation of the cycle stability. This must be of a great advantage in a quick searching of materials. Being encouraged with this conclusion, we tried to evaluate the redox behavior of the spinel type $LiMn_2O_4$ as a function of the cycle number. Fig. 6 shows CVs obtained at different scan rates ($\nu=1$–10 mV/s) with a $LiMn_2O_4$ particle (diameter: ~10 μm) after 200 repeated cycles at 10 mV/s. Fig. 7 shows the enlarged CV of the lowest scan rate, 1 mV/s. It shows excellent reversibility and cycle stability over 200 cycles; lowering of the peak current as observed in the $LiCoO_2$ case was not recognized. There are two well-defined peaks, the first anodic peak potential $E_A=4.01$ V and the second anodic peak potential $E_B=4.12$ V, and for the cathodic peaks, $E_{A'}=3.99$ and $E_{B'}=4.11$ V versus Li/Li^+,

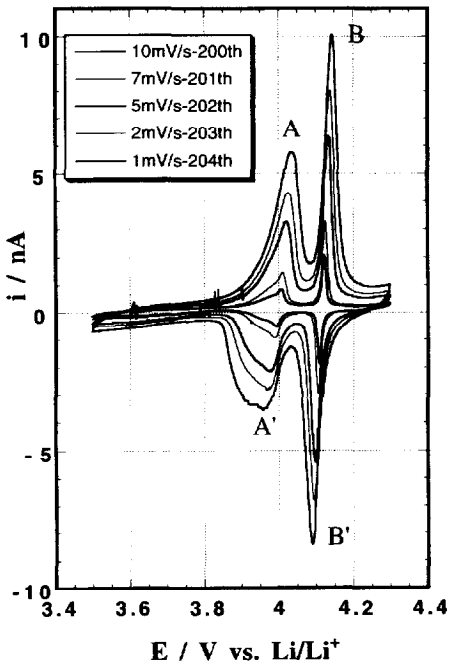

Fig. 6. Cyclic voltammograms for a single particle $LiMn_2O_4$ (diameter: ~10 μm) at various sweep rates in 1 M $LiClO_4$/PC + EC. Those CVs were obtained after 200 repeated potential cycling at 10 mV/s.

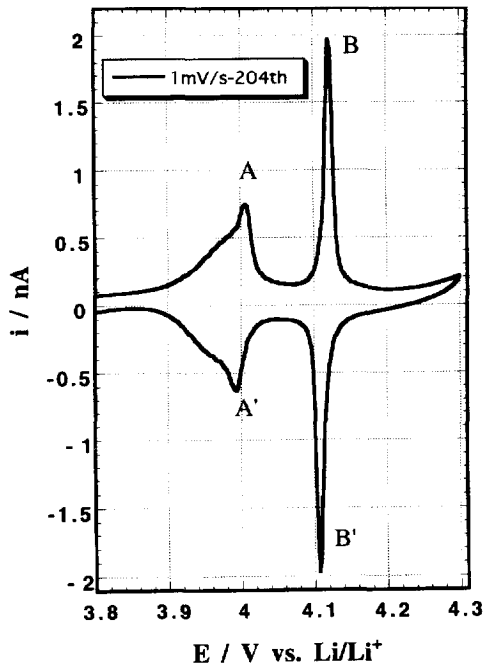

Fig. 7. Cyclic voltammogram for a single particle $LiMn_2O_4$ (diameter: 10 μm) at 1 mV/s in 1 M $LiClO_4$/PC + EC. This CV was obtained after 200 repeated potential cycling at 10 mV/s.

which were determined in Fig. 7. The midpotential between the anodic and cathodic peaks is 3.998 V for the first wave and 4.114 V for the second wave, which can be regarded as

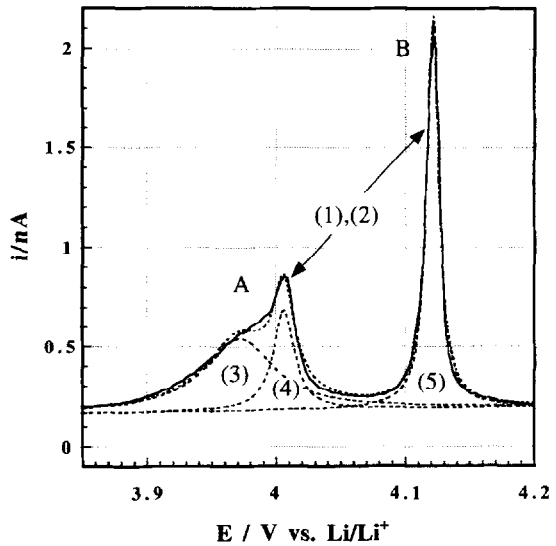

Fig. 8. Deconvolution of the anodic side of the voltammogram schown in Fig. 7. (1, ———) observed; (2, · · ·) fitted; (3, · · ·) deconvoluted; the half peak width $\Delta E_{1/2}=78$ mV; (4, · · ·) deconvoluted, $\Delta E_{1/2}=18$ mV; (5, · · ·) deconvoluted, $\Delta E_{1/2}=11$ mV.

the thermodynamic potential (E^0) of the redox process. It is also noted that the second peak (B) is sharper and larger than those of the first peak (A); the half-peak widths in Fig. 7 are $\Delta E_{A/2}=73$ mV and $\Delta E_{B/2}=12$ mV. The first wave is strange, showing an asymmetric shape with a small peak on the top, which becomes visible with decreasing the sweep rate.

The CV was easily deconvoluted into three waves as shown in Fig. 8, where only the anodic side was depicted. The Lorentz functions were used to fit them. It was shown that the second wave (B) was expressed by a symmetrical curve (the half-peak width, $\Delta E_{B/2}=11.2$ mV), whereas the first wave (A) was deconvoluted into two curves, broad ($\Delta E_{1/2}=78.0$ mV) and sharp ($\Delta E_{1/2}=18.1$ mV) bell-shape curves as expected from the observed shape. According to Ohzuku et al. [25] reporting the changes in lattice parameters during lithium-ion extraction from $Li_xMn_2O_4$, one-phase oxidation takes place for $1.0>x>0.603$ (midpoint potential at 3.94 V) and two-phase oxidation proceeds for $0.60>x>0.27$ (midpoint potential at 4.11 V). Our CV behavior can be explained based on their reaction scheme; the second peak is due to the two-phase oxidation/reduction and the first wave corresponds to the one-phase region. The initial part of the first wave showing slow current increase seems to be just the one-phase oxidation, where the lithium-ion extraction is proceeding in a homogeneous phase (Phase II in Ref. [25]). At the end of this Phase II region, a very sharp, small current peak was observed, which overlapped the first wave of CV. It was separated from the wave (A) as shown by the deconvoluted curve (4) in Fig. 8. The reason of this small peak is not clear at present. However, considering that the current rapidly decreases beyond the top of the first wave, we suppose that the potential region between 4.01 V and the onset potential ($E\sim4.08$ V) of the second peak can be regarded as a transition region from the homogeneous Phase II to the two-phase coexisting region (Phase I). After the transition is completed, then the two-phase oxidation starts at about 4.08 V, resulting in the sharp second wave. Measurements of the second peak currents versus sweep rates relationship showed that i_p was proportional to $v^{0.7-0.8}$, suggesting that the diffusion process is complicated. We need further characterization to confirm the above potential profile of the de-intercalation process, and it is in porgress in this laboratory by using in situ XRD techniques.

It is realized that the microvoltammetric method is very suitable to a rapid searching of new materials and allow us to study kinetic aspects of solid-state electrochemistry.

Acknowledgements

This research was supported by Grand-in-Aid for Scientific Research (No. 06 453 111) of The Ministry of Education, Science and Culture.

References

[1] R.M. Wightman, *Anal. Chem., 53* (1981) 1125A.
[2] M. Fleischmann, S. Pons, D.R. Rolison and P.P. Schimidt, *Ultramicroelectrodes*, Datatech Systems, Scientific Publishers, Morganton, 1987.
[3] S. Pons and M. Fleischmann, *Anal. Chem., 59* (1987) 1391A.
[4] S.A. Campbell, C. Bowes and R.S. McMillan, *J. Electroanal. Chem., 284* (1990) 195.
[5] J.D. Genders, W.M. Hedges and D. Pletcher, *J. Chem. Soc., Faraday Trans. 1, 80* (1984) 3399.
[6] W.M. Hedges and D. Pletcher, *J. Chem. Soc., Faraday Trans. 1, 82* (1986) 179.
[7] K.S. Aojula and D. Pletcher, *J. Chem. Soc. Faraday Trans., 86* (1990) 1851.
[8] M.W. Verbrugge and B.J. Koch, *J. Electroanal. Chem., 367* (1994) 123.
[9] M. Bursell and P. Björnbom, *J. Electrochem. Soc., 137* (1990) 363.
[10] H. Ura, T. Nishina and I. Uchida, *J. Electroanal. Chem., 396* (1995) 169–173.
[11] E.W. Kristensen, W.G. Kuhr and R.M. Wightman, *Anal. Chem., 59* (1987) 1752.
[12] T.K. Chen, Y.Y. Lau, D.K.Y. Wong and A.G. Ewing, *Anal. Chem., 64* (1992) 1264.
[13] C. Amatore, R.S. Kelly, E.W. Kristensen, W.G. Kuhr and R.M. Wightman, *J. Electroanal. Chem., 213* (1986) 31.
[14] W.H. Church and J.B. Justice, Jr., *Anal. Chem., 59* (1987) 712.
[15] J.B. Chien, R.A. Wallingford and A.G. Ewing, *J. Neurochem., 54* (1990) 633.
[16] I. Uchida, T. Abe, T. Itabashi and T. Matsue, *Chem. Lett.*, (1990) 1227.
[17] T. Matsue, S. Koike, T. Abe, T. Itabashi and I. Uchida, *Biochim. Biophys. Acta., 1101* (1992) 69.

[18] T. Nishina, H. Ura and I. Uchida, *J. Electrochem, Soc., 144* (1997) 1273.
[19] M. Sugawara, M. Fujiwara and K. Matsuki, *Prog. Batteries Batteries Mater., 12* (1993) 181.
[20] I. Uchida and H. Sato, *J. Electrochem. Soc., 142* (1995) L139–L141.
[21] J.N. Reimers and J.R. Dahn, *J. Electrochem. Soc., 139* (1992) 2091.
[22] T. Ohzuku and A. Ueda, *J. Electrochem. Soc., 141* (1994) 2972.
[23] D. Ellis, M. Eckhoff and V.D. Neff, *J. Phys. Chem., 85* (1981) 1225–1231.
[24] T. Ohzuku, K. Sawai and T. Hirai, *J. Electrochem. Soc., 132* (1985) 2828–2834.
[25] T. Ohzuku, M. Kitagawa and T. Hirai, *J. Electrochem. Soc., 137* (1990) 769–775.